Sputter-induced grain boundary junctions in $YBa_2Cu_3O_{7-x}$ thin films on MgO

B. V. Vuchic and K. L. Merkle
Materials Science Division and Science and Technology Center for Superconductivity, Argonne National Laboratory, Argonne, Illinois 60439

K. A. Dean, D. B. Buchholz, R. P. H. Chang, and L. D. Marks
Department of Materials Science and Engineering and Science and Technology Center for Superconductivity, Northwestern University, Evanston, Illinois 60208

(Received 12 August 1994; accepted for publication 28 November 1994)

A low voltage argon ion sputter technique was used to form grain boundary junctions in $YBa_2Cu_3O_{7-x}$ thin films on MgO. The $YBa_2Cu_3O_{7-x}$ thin film grown on a pre-sputtered region of MgO was rotated 45° about the [001] axis relative to the $YBa_2Cu_3O_{7-x}$ thin film grown on an adjacent unsputtered region of the substrate. $YBa_2Cu_3O_{7-x}$ thin films were grown using pulsed organometallic beam epitaxy (POMBE). The current-voltage and resistance-temperature characteristics of individual grain boundary junctions demonstrated weak-link-type behavior. Sputter-induced 45° grain boundary junctions are advantageous in device applications because they are planar and simple to form in many configurations. © *1995 American Institute of Physics.*

I. INTRODUCTION

Most high-angle grain boundaries in high-temperature superconductors are weak links.[1] Weak links are detrimental for high-power applications; however, if controlled properly grain boundaries can be used as Josephson junctions for microelectronic device applications such as SQUIDs. Reproducibility of the grain boundary transport characteristics and the ability to integrate the junctions into device circuits are the critical issues for commercial applications of these grain boundary junctions. A variety of techniques are used in forming grain boundary junctions: bicrystal,[2,3] biepitaxial,[4,5] substrate modification[6] and step-edge junctions.[7,8] All of these techniques are based on formation of epitaxial thin films.

MgO is often used as a substrate material in growth of $YBa_2Cu_3O_{7-x}$ thin films. The various possible epitaxial orientation relationships between $YBa_2Cu_3O_{7-x}$ and MgO are described in many studies.[9–11] The most common epitaxial orientation relationship observed is $YBa_2Cu_3O_{7-x}$ [001]‖MgO [001] and $YBa_2Cu_3O_{7-x}$ [110]‖MgO [110]. One other type of orientation relation often seen is $YBa_2Cu_3O_{7-x}$ [001]‖MgO [001] and $YBa_2Cu_3O_{7-x}$ [100]‖MgO [110]. Previous work has shown that under suitable conditions ion beam modification of the substrate could induce the latter orientation,[6] however this result was not reproducible, probably due to variations in the growth conditions.[12] In this report we describe the development of a simple ion beam substrate modification technique which is used in conjunction with pulsed organometallic beam epitaxy (POMBE) to reproducibly form controlled regions of 45° rotated $YBa_2Cu_3O_{7-x}$ thin films on MgO. A portion of a MgO substrate is sputter treated prior to thin film growth. Epitaxial thin films were grown using specific growth conditions.[13] The film grown on the sputtered portion of the substrate is rotated by 45° about the [001] axis relative to the untreated portion of the substrate. The rotation in the thin film occurred consistently using various ion beam energies and irradiation times as described below.

II. EXPERIMENT

Commercially polished single crystal [100] MgO substrates were used. The substrate was physically masked using either a contact mask or using hardbaked photoresist. The substrate was then sputtered using a low voltage 3-cm-diam beam Kaufman-type ion source. Argon ions were used at a range of energies from 100 to 500 eV. The beam current density was approximately 1 mA/cm^2. The angle of incidence of the ion beam onto the substrate was 90° (normal to the substrate surface). The substrate was mounted with good thermal contact to a copper stage, and irradiated at room temperature. The background pressure during irradiation was 2×10^{-4} Torr. The physical mask was then removed, or the photoresist was dissolved in acetone. Typical step heights for a 2 min irradiation at 200 eV were 10–20 nm as determined by profilometry.

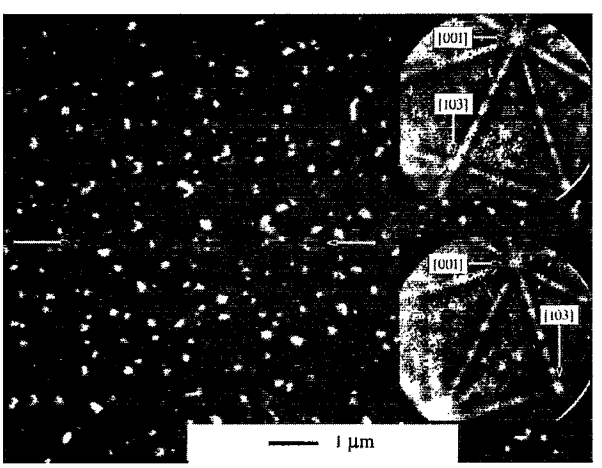

FIG. 1. Scanning electron micrograph of the grain boundary region (indicated by the arrows) in the $YBa_2Cu_3O_{7-x}$ thin film. Insets a and b show the thin film orientation on either side of the grain boundary using corresponding electron backscatter Kikuchi patterns of the film.

 0021-8979/95/77(6)/2591/4/$6.00

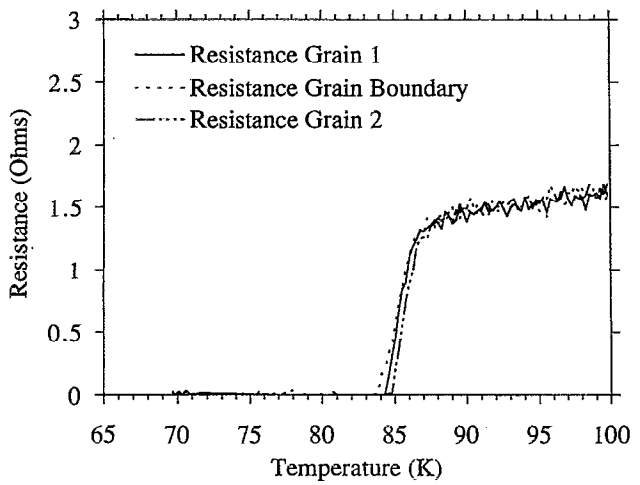

FIG. 2. Resistance vs temperature curve of the $YBa_2Cu_3O_{7-x}$ grain on the presputtered and the unsputtered portion of the substrate and the grain boundary region.

The thin films were grown using a pulsed organometallic beam epitaxy technique (POMBE) for *in situ* $YBa_2Cu_3O_{7-x}$ deposition described in more detail elsewhere.[13] This technique allowed controlled slow growth at relatively low growth temperatures. The substrate was held at approximately 700 °C during growth. The thin film growth was assisted by an oxygen plasma. With the oxygen plasma activated, the substrate was held at the growth temperature for at least 30 min prior to thin film growth. The ambient gas in the growth chamber during deposition was approximately 70% oxygen, 28% helium, and 2% water vapor. The deposition rates of the films varied from 3 to 11 Å/min. The film thicknesses were between 2100 and 3000 Å.

After deposition, the orientation of the film was determined with backscatter electron Kikuchi patterns in a JEOL 6400 scanning electron microscope (SEM) (see Fig. 1).[14] The scanning electron microscope (SEM) was also used to study the film morphology. Standard transmission electron microscopy sample preparation techniques were applied to make plan view samples. A 3 mm diameter disk was cut with an ultrasonic disk cutter. The sample was thinned by mechanically grinding to 120 μm thickness. After thinning, the sample was dimpled to 25 μm and ion milled to perforation. Microstructural analysis was performed using a Phillips CM30 transmission electron microscope (TEM) at 100 kV. High-resolution electron microscopy (HREM) of the grain boundaries was performed using a JEOL 4000 EXII operated at 200 kV, in order to reduce beam damage.

Low-temperature four-probe transport measurements were made to determine current-voltage and resistance-temperature characteristics. The samples were patterned for transport measurements with a molybdenum contact mask with a 35-μm-wide microbridge. Argon ion milling was used to remove the exposed regions of the thin film. The microbridge allowed for independent transport measurement across the grain boundary as well as in the two adjacent grains. The contact pads were cleaned with a low-energy ion

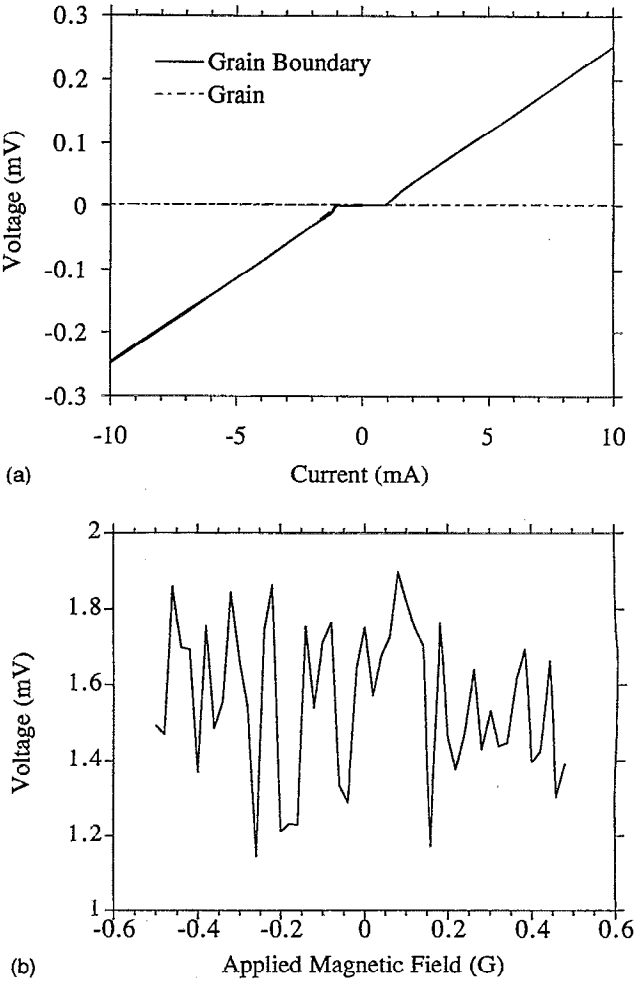

FIG. 3. (a) Current-voltage characteristics of the $YBa_2Cu_3O_{7-x}$ grain and grain boundary at 5 K. (b) The voltage offset of the grain boundary, using a constant current, as a function of applied magnetic field (parallel to the grain boundary) at 70 K.

beam and then silver contacts were evaporated *in situ*. The samples were then annealed at 430 °C for 5 h in flowing ultrahigh purity oxygen. Gold leads were connected to the sample using silver paint. Standard four-probe measurements were performed in a cold finger flow cryostat. A 1 μV criteria was used in determining the critical current from the current-voltage (I-V) measurements.

III. RESULTS AND DISCUSSION

After thin film growth the orientation of the $YBa_2Cu_3O_{7-x}$ thin film was determined with backscattered electron Kikuchi patterns (see Fig. 1). This technique allowed nondestructive local determination of the orientation with approximately 0.5 μm lateral resolution. The $YBa_2Cu_3O_{7-x}$ grown on the unsputtered MgO had the orientation relation of $YBa_2Cu_3O_{7-x}$ [001]‖MgO [001] and $YBa_2Cu_3O_{7-x}$ [110]‖MgO [110]. On the pre-milled portion of the substrate, the film grew predominantly with the orientation rotated 45° about the [001] axis: $YBa_2Cu_3O_{7-x}$ [001]‖MgO [001] and $YBa_2Cu_3O_{7-x}$ [110]‖MgO [100].

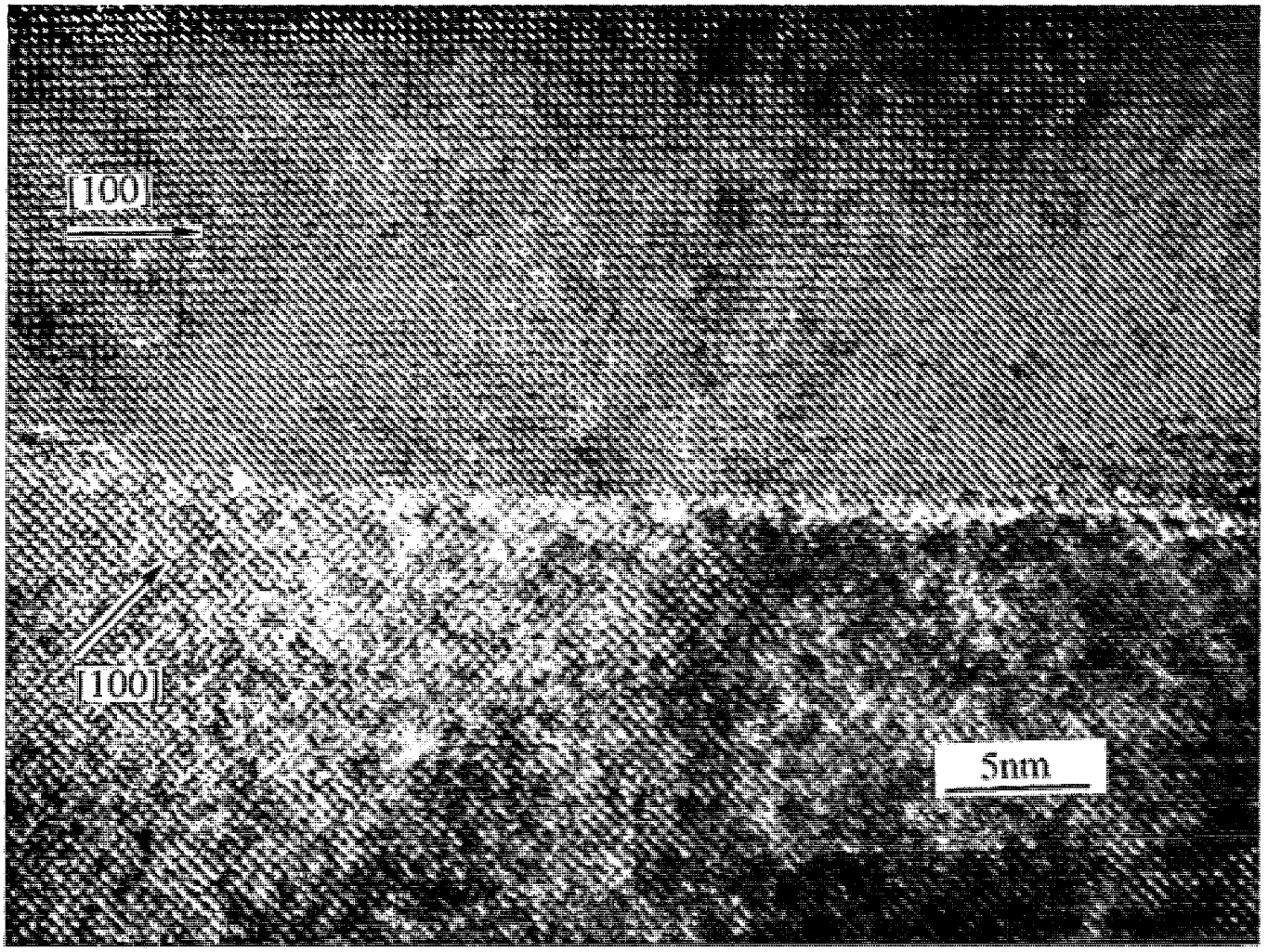

FIG. 4. High-resolution electron micrograph showing long straight asymmetric facets along the grain boundary.

Backscattered Kikuchi patterns indicated the samples had a 45° rotation about the $YBa_2Cu_3O_{7-x}$ [001] across the entire ion irradiated region. The ion irradiation pretreatment successfully induced rotations for ion energies as low as 100 eV. We do not expect the transport properties to be dependent on the ion energies used, however, we have not yet verified this experimentally. Lowering the ion energies may be of considerable importance for planar technologies by minimizing the step height or possibly eliminating the step altogether. Possible mechanisms for the modified epitaxy are currently under investigation.

Across the whole film, within both rotated and unrotated regions, there were a few individual grains which had different orientations constituting less than 5% of the total grain region. Moreover, in a region approximately 2 μm wide at the border between the sputtered and unsputtered substrate, a combination of the rotated and unrotated grains were sometimes found mixed together. The junction region therefore did not necessarily consist of one pristine grain boundary.

Invariably the transport measurements showed weak-link type behavior. In contrast to other techniques used to form grain boundary junctions, the weak link is not inherently dependent on the formation of a step in the substrate. Therefore, the sputter induced junctions are compatible with planar device technology.

The resistance-temperature characteristics of a typical sample are shown in Fig. 2. The junction exhibits a very slight decrease in T_c (1 K) relative to the grain. The two grains also have small differences in T_c (0.5 K). Within the sensitivity of the measurement, the transition region does not show a foot structure as is sometimes seen in grain boundary junctions.[15] The grain boundary current-voltage characteristics [see Fig. 3(a)] demonstrate typical weak-link behavior. The critical current density of the grain boundary is significantly reduced compared to the two adjacent grains. The critical current density across the grain boundary is 1.4×10^4 A/cm^2 at 5 K. The grain boundary has an I_cR_n product $=25.5$ μV. The critical current densities of the adjacent grains were not measured beyond what is shown in Fig. 3(a) due to the possibility of destroying the grain boundary junction from resistive heating above the critical current. Figure 3(b) depicts the voltage as a function of applied magnetic field perpendicular to the thin film (parallel to the grain boundary) at 70 K with a constant dc current through the sample. Strong oscillations of the critical current were observed as a function of applied magnetic field. This behavior

has been previously observed in other grain boundary junctions[16,17] and can be attributed to inhomogeneity of the Josephson coupling strength across the junction. The varying critical current dependence as a function of applied magnetic field can be related to the width of the junction.[18]

The microstructure of the grain boundary was analyzed using high-resolution electron microscopy of plan view samples. The grain boundary showed long straight facets which were well structured up to the grain boundary (see Fig. 4). The grain boundary had microfacets which were asymmetric with the orientation of $YBa_2Cu_3O_{7-x}$ [100] or $YBa_2Cu_3O_{7-x}$ [010]‖$YBa_2Cu_3O_{7-x}$ [110]. No second phase or precipitation was observed along the grain boundary. Some regions of the grain boundary were slightly inclined relative to the substrate normal. In comparison to the microstructure of biepitaxial grain boundaries,[19] the grain boundaries on MgO were more uniform in their structure. In the grain boundaries on the MgO the structural integrity was maintained up to the grain boundary whereas the biepitaxial junctions were often structurally distorted within 1 nm of the boundary. The long straight facets suggest that there is better electrical connectivity between the grains, thus improving current transport across the grain boundary.

The low-voltage ion beam modification technique provides several advantages over other methods in forming weak-link junctions. The major advantage of the technique is its simplicity. This technique can be easily integrated into planar thin film technology. By using suitable masking techniques the junctions can be placed anywhere on the substrate. By reducing the ion energy to 100 eV and the irradiation time to 2 min damage to the substrate can be minimized. Moreover, the step height in the MgO under these conditions would be extremely small causing little distortion in the substrate topology. This would be particularly important for producing multilayered devices.

IV. CONCLUSION

A method for the controlled introduction of 45° [001] grain boundaries in $YBa_2Cu_3O_{7-x}$ thin films on MgO has been developed. The low-voltage argon ion technique has been shown to work for many incident ion energies and irradiation times. The junctions formed exhibited weak-link type of transport behavior. The structure of the grain boundaries was dominated by straight asymmetric facets free of second phases or precipitates. This technique has proven to be a simple way of forming controlled grain boundary junctions and may be applicable to forming integrated Josephson junctions in microelectronic devices.

ACKNOWLEDGMENTS

We thank J. W. Funkhouser for his assistance with some low-temperature measurements. This work was supported by the National Science Foundation Office of Science and Technology Centers, under contract #DMR 91-20000 (BVV, KAD, DBB, RPHC, and LDM) and the U.S. Department of Energy, Basic Energy Sciences-Materials Science (KLM), under contract #W-31-109-ENG-38.

[1] D. Dimos, P. Chaudhari, J. Mannhart, and F. K. LeGoues, Phys. Rev. Lett. **61**, 219 (1988).
[2] D. Dimos, P. Chaudhari, and J. Mannhart, Phys. Rev. B **41**, 4038 (1990).
[3] Z. G. Ivanov, P. A. Nilsson, D. Winkler, J. A. Alarco, T. Claeson, E. A. Stepantsov, and A. Y. Tzalenchuk, Appl. Phys. Lett. **59**, 3030 (1991).
[4] K. Char, M. S. Colclough, S. M. Garrison, N. Newman, and G. Zaharchuk, Appl. Phys. Lett. **59**, 733 (1991).
[5] K. Char, M. S. Colclough, L. P. Lee, and G. Zaharchuk, Appl. Phys. Lett. **59**, 2177 (1991).
[6] N. G. Chew, S. W. Goodyear, R. G. Humphreys, J. S. Satchell, J. A. Edwards, and M. N. Keene, Appl. Phys. Lett. **60**, 1516 (1992).
[7] K. P. Daly, W. D. Dozier, J. F. Burch, S. B. Coons, R. Hu, C. E. Platt, and R. W. Simon, Appl. Phys. Lett. **58**, 543 (1991).
[8] C. L. Jia, B. Kabius, K. Urban, K. Herrmann, G. J. Cui, J. Schubert, W. Zander, A. I. Braginski, and C. Heiden, Physica C **175**, 543 (1991).
[9] S. McKernan, M. G. Norton, and C. B. Carter, J. Mater. Res. **7**, 1052 (1992).
[10] D. M. Hwang, T. S. Ravi, R. Ramesh, S. -W. Chan, C. Y. Chen, L. Nazar, X. D. Wu, A. Inam, and T. Venkatesan, Appl. Phys. Lett. **57**, 1690 (1990).
[11] D. H. Shin, J. Silcox, S. E. Russek, D. K. Lathrop, B. Moeckly, and R. A. Buhrman, Appl. Phys. Lett. **57**, 508 (1990).
[12] N. G. Chew (private communication).
[13] D. B. Buchholz, S. J. Duray, D. L. Schulz, T. J. Marks, J. B. Ketterson, and R. P. H. Chang, Mater. Chem. Phys. **36**, 377 (1994).
[14] J. A. Venables and C. J. Harland, Philos. Mag. **27**, 1193 (1973).
[15] R. Gross. P. Chaudhari, D. Dimos, A. Gupta, and G. Koren, Phys. Rev. Lett. **64**, 228 (1990).
[16] P. Chaudhari, J. Mannhart, D. Dimos, C. C. Tsuei, J. Chi, M. M. Oprysko, and M. Scheuermann, PRL **60**, 1653 (1988).
[17] D. K. Lathrop, B. H. Moeckly, S. E. Russek, and R. A. Buhrman, Appl. Phys. Lett. **58**, 1095 (1991).
[18] P. A. Rosenthal, M. R. Beasley, K. Char, M. S. Colclough, and G. Zaharchuk, Appl. Phys. Lett. **59**, 3482 (1991).
[19] B. V. Vuchic and K. L. Merkle (unpublished).